ALLEN INSTITUTE for BRAIN SCIENCE

Allen Cell Types Database

TECHNICAL WHITE PAPER: OVERVIEW

OVERVIEW

The constituent elements of cortex are neurons and their supporting actors - astrocytes, oligodendrocytes and microglia, as well as the vasculature. Given our interest in understanding perception and sensory-motor action that takes place at the 1 second time scale, we focus here on nerve cells, of which there are about 16 billion in the human cortex and 14 million in the mouse (Herculano-Houzel 2009). These neurons can be classified into distinct types based on their dendritic morphology and axonal projections, their physiological and functional behavior and the genes that they express.

The idea that neuronal cell types have functional relevance is best documented in the vertebrate retina, where around 70 functionally distinct cell types have been reported and described using a combination of receptive field properties, cell morphology, cellular location within the retina, electrophysiology, connectivity and, more recently, gene expression. These neural components combine to process the rain of incoming photons into action potentials that leave the retina along the optic nerve (Masland 2012). Since the earliest anatomical studies of Ramón y Cajal and Camillo Golgi, it has been evident that there is likewise a plethora of neural types in the cerebral cortex (Cauli *et al*., 1997, 2000; Toledo-Rodriguez *et al*., 2004; Sugino *et al*., 2006; Petilla *et al*., 2008; Thomson 2010; DeFelipe *et al*., 2013). The total number is unclear but could be as high as 1000 cell types, inferred from the tiling principle, the hypothesis that the dendritic footprint of any one cell type must cover the entire surface of cortex at least once (Crick 1994; Stevens 1998).

Yet despite much effort, there is no consensus on how many cortical cell types exist, whether they tile the cortical surface, how any cell type varies across the cortical sheet and among different species, or even whether every cell in the adult neocortex can be unambiguously assigned to a unique cell class. One limiting factor has been combining the findings across individual studies and laboratories due to differences in preparations. An additional limitation has been the availability of tools for repeatedly targeting groups of neurons. With the recent proliferation of Cre lines that label genetically-defined subsets of neurons within the cortex and the thalamus, we now have the tools to reproducibly target and probe distinct neural populations across experiments. These tools will also allow us to correlate neural class diversity with functionally described cell classes obtained in other Allen Institute projects.

The initial goals of the Allen Institute's cell type project is to characterize, in a systematic and standardized manner, individual neurons in the dorsal part of the lateral geniculate complex (LGd) and the primary visual cortex (VISp or V1) of the young adult laboratory mouse at its most basic level: intrinsic electrophysiology properties, neuron morphology, transcriptional profile, and parameters from multiple computational models incorporating one or more of these experimentally defined modalities. Through clustering and correlational analyses of these different types of data, we wish to establish a database of distinct neuronal cell types in VISp and LGd.

The current main components of data generation and analysis include electrophysiology, morphology, transcriptomics, and modeling (**Figures 1** and **2**). In more detail, the four distinct components are: (i) an

electrophysiological characterization of the biophysical and intrinsic firing properties of these cells, based on somatic patch recordings in slices, (ii) image data and morphological reconstructions of the dendritic tree and the initial part of the axon within the slice based on biocytin fills through the patch pipettes, (iii) transcriptomics data obtained from single cells enriched by Cre-driven labeling and fluorescence-guided cell selection by FACS, and (iv) a variety of abstract point models (*generalized, leaky integrate-and-fire* or GLIF models) and more biophysical active compartmental models of these neurons. Using many of the same transgenic mouse lines that have been utilized in the Allen Mouse Brain Connectivity Atlas, this database will add single cell resolution and additional data modalities to our existing population-level connectivity and gene expression atlases.

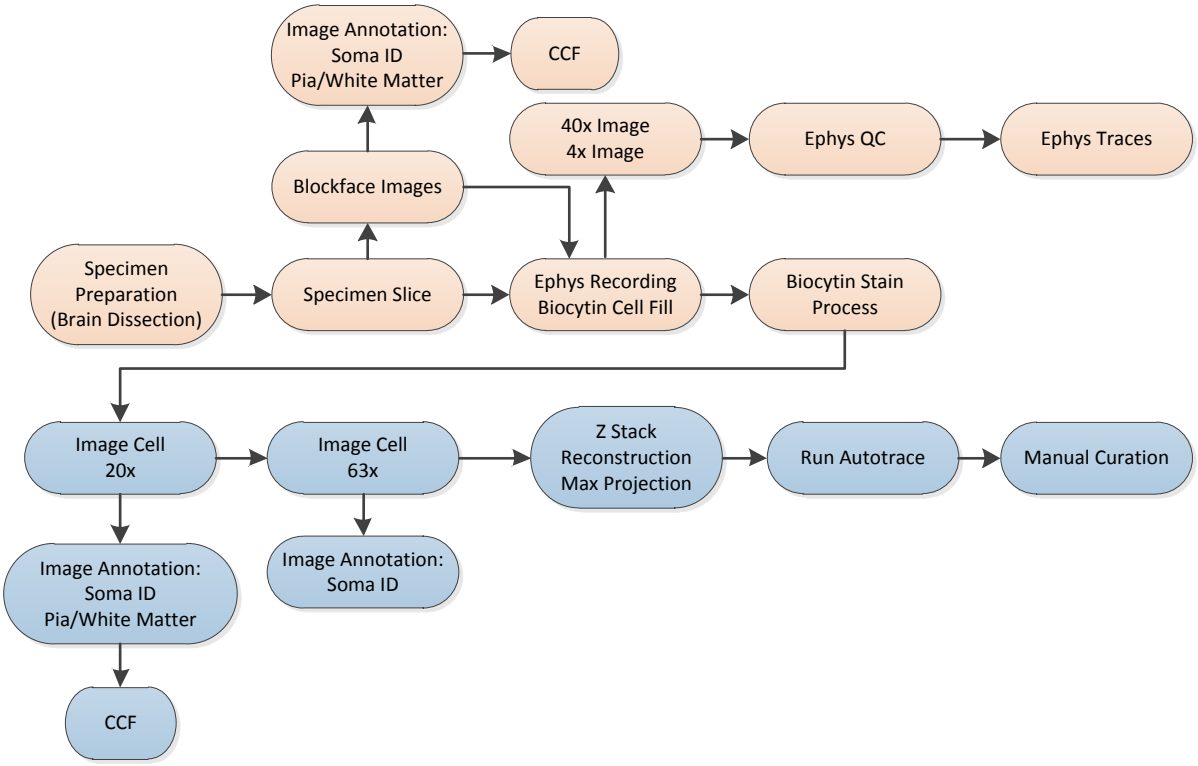

Figure 1. Overview of the electrophysiology and morphology data generation workflow.
Tissue enters the pipeline from a transgenic mouse line. The brain is then dissected and sliced, followed by electrophysiology recording and filling of the neuron of interest with biocytin. Biocytin-filled neurons are then processed for imaging and morphological reconstruction. Data from each modality are integrated into modeling and classification.

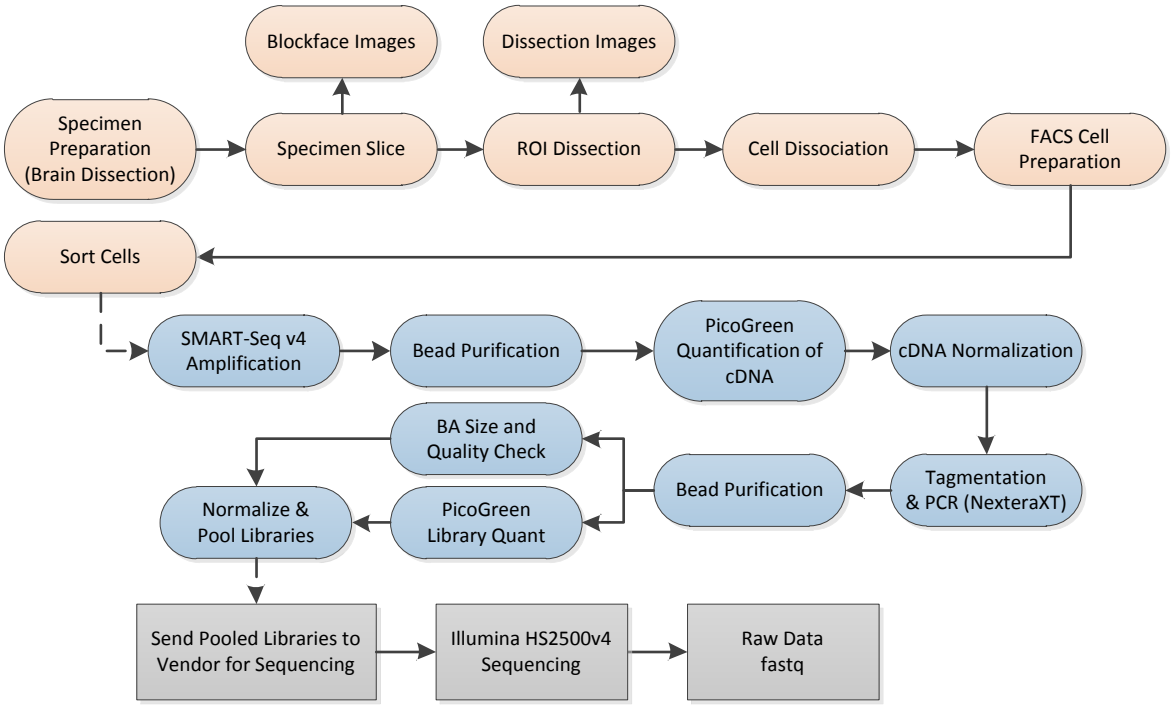

Figure 2. Overview of the transcriptomics workflow for RNA-Seq data generation.
The main components of the workflow for transcriptomics data generation include brain dissection, Region of Interest (ROI) dissection, cell sorting, and RNA amplification and library preparation for RNA-Seq. Following data processing and quality control assessment, the single-cell data was clustered into groups using a consensus approach based on iterative clustering techniques.

Electrophysiology

Slices are prepared from P45 to P70, male and female mice (either an interneuron or layer specific Cre driver line crossed to an Ai14 tdTomato reporter line). Slices (350 µm) are sectioned using a vibrating microtome: each slice is imaged to aid in brain region identification and registration to the Allen Mouse Common Coordinate Framework (CCF). For more information on the CCF, see the whitepaper located in the Documentation tab. Whole cell current clamp recordings are made from identified, tdTomato-positive neurons or nearby tdTomato-negative neurons for a subset of the experimental data. Stimulation waveforms are designed to: 1) interrogate intrinsic membrane properties that contribute to the input/output function of neurons, 2) understand aspects of neural response properties *in vivo*, and 3) construct and test computational models of varying complexity emulating the neural response to stereotyped stimuli. Stimulus sets are divided into 2 groups: a rigid 'Core 1' sequence designed to establish baseline properties that is applied to every neuron, and a more flexible 'Core 2' sequence that can be tailored to each Cre line and is influenced by close feedback from modelers and *in vivo* recordings. For more information on the Electrophysiology experiments, see the Electrophysiology whitepaper in the Documentation tab. Electrophysiology data are reported with metadata detailing experimental conditions such as electrode resistance, tight seal resistance, and series resistance, as well as more granular details such as bath temperature and amplifier settings on a sweep by sweep basis. Data QC are based on cell-wide and sweep-based criteria.

Morphology

Three-dimensional (3D) reconstructions of the soma, dendrites and the initial part of the axon and/or the full axon are generated for a subset of neurons with good quality electrophysiology and good biocytin fill. These reconstructions are used for biophysical modeling and neuron classification efforts. 3D reconstructions are generated based on an image stack. High resolution image stacks of biocytin filled neurons are first evaluated for the likelihood that the morphology will result in a high quality neuronal reconstruction. For more information on the Morphological reconstruction, see the Morphology whitepaper in the Documentation tab. Prioritized neurons then enter a Vaa3D-based (Peng *et al*. 2010) image processing and reconstruction pipeline. The

process begins with a color inversion and a variable enhancement of the signal to noise ratio in the image (Zhou *et al*., 2014). The enhanced image is then used to generate an automated reconstruction of the neuron with the Neuron Crawler tool (Zhou *et al*., 2015). The automated reconstructions are then extensively manually corrected and curated using a range of tools in Vaa3D, *e.g.*, virtual finger, polyline, assemble neuron live, delete and type multiple branches by stroke. These features are then used for morphological analyses.

Transcriptomics

Slices are prepared from (P53-P59) male transgenic mice (either an excitatory, pan-neuronal or inhibitory Cre driver line crossed to an Ai14 tdTomato reporter line). A blockface image is acquired to aid in brain region identification and registration to the CCF before each section is sliced at 250 µm intervals using a vibrating microtome. Regions of interest are microdissected and dissected tissue pieces are treated with protease and subsequently triturated. From this cell suspension, single cells are isolated by fluorescence-activated cell sorting (FACS). After sorting, cDNA amplification and library construction is performed using SMART-Seq v4 (Clontech) and Nextera XT (Illumina) kits. Single cell libraries are sequenced on HiSeq (Illumina) to generate 50 base-pair paired-end reads. Raw read (fastq) files are aligned to the mm10 mouse genome sequence (Genome Reference Consortium, 2011) with the RefSeq transcriptome version GRCm38.p3 (current as of 01/15/2016). Transcriptome alignment is performed using RNA-Seq by Expectation-Maximization RSEM (Li *et al.*, 2011). Reads that did not map to the transcriptome are then aligned to the mm10 genome sequence using Bowtie with default settings (Langmead et al., 2009). Reads that mapped to neither the transcriptome with RSEM or to the genome with Bowtie are mapped against the ERCC sequences. After alignment, quality control is performed, followed by clustering the single cell data into groups using a consensus approach based on two iterative clustering techniques - iterative weighted gene co-expression network analysis (WGCNA) (as described in Tasic *et al.*, 2016) and an iterative version of Seurat (as described in Macosko *et al*., 2015). For more information on the transcriptomics data generation, see the Transcriptomics whitepaper in the Documentation tab.

GLIF Models

For simulations of neural networks there is a tradeoff between the size of the network that can be simulated and the complexity of the model used for individual neurons. Generalized leaky integrate-and-fire models reduce synaptic integration occurring in the extended dendritic tree to a simple linear process whose output is compared to a single firing threshold. If the threshold is exceeded, a spike is generated and the internal variables are reset. A series of models of increasing complexity aimed at reproducing the spiking behavior of recorded neurons are being constructed. Starting with leaky integrate and fire model, three mechanisms are added: afterspike currents, reset rules in which membrane potential and threshold after a spike depend on the electrical state prior to the spike and voltage dependent changes in threshold (Koch 1999; Pozzorini *et al*. 2015). Electrophysiological stimuli are designed to specifically estimate some of the parameters present in the generalizations. Following this initial estimate some parameters are further tuned to optimize the reproduced spike times on a training noise stimulus. More precisely, we maximize the likelihood of a model neuron with intrinsic noise to reproduce exactly the observed spike train. The model performance is subsequently evaluated on a test stimulus: for different time scales the fraction of the variance of the neuronal response, which is explained by the model, is computed. For more information on the GLIF Models, see the whitepaper in the Documentation tab.

Biophysical Models

The experimental data from cortical neurons in slice preparations is utilized to construct biophysically detailed models of individual cells (Koch 1999). For such biophysically-detailed, compartmental models we account for the neural morphology and emulate electrophysiological responses in two setups: (1) by assuming active conductances at the soma, with the rest of the neuron remaining passive, and (2) by assuming active conductances along the entirety of the neural morphology (all-active). These models are constructed only for those neurons for which both high-quality electrophysiological recordings and intact dendritic morphological reconstructions are obtained. To build a model for each cell, a genetic optimization algorithm is used in the in-house high-performance computing setting, taking advantage of repeated single-cell simulations with the program NEURON (Hines and Carnevale, 1997) and directed evolution of biophysical parameters, following the approach of Segev and colleagues (Druckmann *et al*., 2007; Hay *et al*., 2011). For setup (2), a genetic optimization algorithm is used on a Blue Gene Q supercomputer located in Lugano (Switzerland) for the

development of all-active models with algorithms, workflows, and analyses following (Druckmann *et al*., 2007; Hay *et al*., 2011) adapted for the experimental protocols in collaboration with the Blue Brain Project. A model's performance is evaluated by comparing the model and experimental values of specific electrophysiological features computed from the somatic voltage response to somatic current injection (including frequency of firing in response to a step current injection, average action potential peak values, average width of action potentials, and several others). For more information on the Biophysical Models, see the whitepapers in the Documentation tab.

Allen Cell Types Database
The data are publicly available online via the Allen Brain Atlas data portal (www.brain-map.org) and are fully integrated with the other Allen Brain Atlas resources.

The Allen Cell Types Database currently includes:

- **Datasets**
  - Electrophysiology: whole cell current clamp recordings made from identified, fluorescent Cre-positive neurons or nearby Cre-negative neurons.
  - Morphology: reconstruction-quality, 3D images of the complete structure of neurons filled and recorded from *in vitro* slice preparations and 3D reconstructions of the dendrites and the initial part of the axon and/or the full axon of each neuron.
  - Generalized Leaky Integrate-and-Fire (GLIF) models: a series of point neuron models of increasing complexity to reproduce the spiking behaviors of the recorded neurons. Starting with a leaky integrate and fire model, more complex models attempt to model variable spike threshold, afterspike currents, and threshold adaptation.
  - Biophysical-Perisomatic models: compartmental model of neurons that account for the neural morphology and emulate electrophysiological responses by assuming biophysically detailed mechanisms for specific families of ionic conductances, with passive dendrites and active conductances at the soma.
  - Biophysical-All Active models: compartmental model of neurons that account for the neural morphology and emulate electrophysiological responses by assuming biophysically detailed mechanisms for specific families of ionic conductances, with active conductances everywhere.
  - Transcriptomics: single-cell RNA-Sequencing with SMART-Seq v4 on fluorescent Cre-positive neurons enriched by FACS.

Mice
Interneuron-specific or layer-specific Cre driver lines for electrophysiology, morphology and modeling, or excitatory, pan-neuronal or inhibitory Cre driver lines for transcriptomics (see **Table 1**) are combined with the universally expressing Cre-dependent responder line, Ai14 (tdTomato) (see **Table 2**) (Madisen *et al*., 2010). Mice are group-housed (5 per cage) in micro ventilated cages with a 12 h light/dark cycle. Purina Lab diet 5001 mouse food and water are given *ad libitum*. The Cre mice are backcrossed to C57BL/6J mice to minimize genetic variance.

Table 1. Cre transgenic lines that are the source of single cells for the Allen Cell Types Database.

Driver Line (Alias)	Originating Lab or Donating Investigator	Public Repository (Stock #)	Official Strain Name	Expression Pattern Summary
Ctgf-2A-dgCre	Allen Institute for Brain Science	The Jackson Laboratory (028535)	B6.Cg-*Ctgf*$^{tm1.1(folA/cre)Hze}$/J	Cre expression is restricted to layer 6b of cortex and in restricted populations within cortical subplate.
Cux2-CreERT2	Ulrich Mueller	MMRRC (032779)	B6(Cg)-*Cux2*$^{tm3.1(cre/ERT2)Mull}$/Mmmh	Enriched in cortical layers 2/3/4, thalamus, midbrain, pons, medulla and cerebellum.

Driver Line (Alias)	Originating Lab or Donating Investigator	Public Repository (Stock #)	Official Strain Name	Expression Pattern Summary
Gad2-IRES-Cre	Z. Josh Huang	The Jackson Laboratory (010802)	STOCK *Gad2*$^{tm2(cre)Zjh}$/J	Specific to GABAergic neurons. Enriched in striatum, piriform cortex, and in restricted populations in thalamus, hypothalamus, cerebellum, olfactory areas, and GABAergic interneurons of cortex.
Htr3a-Cre_NO152	Nathaniel Heintz and Charles Gerfen	MMRRC (036680)	STOCK Tg(Htr3a-cre)NO152Gsat/Mmucd	Reporter expression detected in subset of cortical interneurons. Enrichment is also detected in restricted populations in olfactory areas, pallidum, hypothalamus, pons, medulla, and cerebellum.
Nr5a1-Cre (Sf1-Cre)	Bradford Lowell	The Jackson Laboratory (006364)	FVB-Tg(Nr5a1-cre)2Lowl/J	Expressed in restricted populations within the hypothalamus (ventromedial hypothalamus), and in cortical layer 4.
Ntsr1-Cre_GN220	Nathaniel Heintz and Charles Gerfen	MMRRC (030648)	B6.FVB(Cg)-Tg(Ntsr1-cre)GN220Gsat/Mmucd	Specific to cortical layer 6 neurons.
Pvalb-IRES-Cre	Silvia Arber	The Jackson Laboratory (008069)	B6;129P2-*Pvalb*$^{tm1(cre)Arbr}$/J	Expressed in restricted and/or sparse populations within the cerebellum, medulla, pons, midbrain, cortex, hippocampus, thalamus, and striatum.
Rbp4-Cre_KL100	Nathaniel Heintz and Charles Gerfen	MMRRC (031125)	STOCK Tg(Rbp4-cre)KL100Gsat/Mmucd	Enriched in cortical layer 5 and dentate gyrus.
Rorb-IRES2-Cre	Allen Institute for Brain Science	The Jackson Laboratory (023526)	B6;129S-*Rorb*$^{tm1.1(cre)Hze}$/J	Strong expression in zonal layer of superior colliculus and thalamus subregions. Dense, patchy expression in layer 4 and sparse expression in layers 5, 6 in cortex. Expressed in trigeminal nucleus and small patches of cells in cerebellum.
Scnn1a-Tg2-Cre	Allen Institute for Brain Science	The Jackson Laboratory (009112)	B6;C3-Tg(Scnn1a-cre)2Aibs/J	Reporter expression in sparse and/or restricted regions of cortex (layer 4), thalamus, midbrain, medulla, pons, and cerebellum.
Scnn1a-Tg3-Cre	Allen Institute for Brain Science	The Jackson Laboratory (009613)	B6;C3-Tg(Scnn1a-cre)3Aibs/J	Enriched in cortical layer 4 and in restricted populations within cortex, thalamus, and in cerebellum.
Slc17a6-IRES-Cre (VGLUT2-ires-Cre)	Bradford Lowell	The Jackson Laboratory (016963)	STOCK *Slc17a6*$^{tm2(cre)Lowl}$/J	Widespread expression throughout most of brain, except very sparse expression in striatum and restricted populations within cerebellum, medulla, and pons.
Slc32a1-IRES-Cre (VGAT-ires-Cre)	Bradford Lowell	The Jackson Laboratory (016962)	STOCK *Slc32a1*$^{tm2(cre)Lowl}$/J	Specific to GABAergic neurons. Enriched in striatum and in restricted populations in thalamus, hypothalamus, cerebellum, olfactory areas, and GABAergic interneurons of the cortex.
Snap25-IRES2-Cre	Allen Institute for Brain Science	The Jackson Laboratory (023525)	B6;129S-*Snap25*$^{tm2.1(cre)Hze}$/J	Strong widespread expression throughout the brain.

Driver Line (Alias)	Originating Lab or Donating Investigator	Public Repository (Stock #)	Official Strain Name	Expression Pattern Summary
Sst-IRES-Cre	Z. Josh Huang	The Jackson Laboratory (013044)	STOCK *Sst*$^{tm2.1(cre)Zjh}$/J	Strong scattered expression throughout brain. Localized areas of enrichment include restricted populations in thalamus, amygdala, midbrain, hindbrain, cortical subplate, Purkinje cell layer.
Vip-IRES-Cre	Z. Josh Huang	The Jackson Laboratory (010908)	STOCK *Vip*$^{tm1(cre)Zjh}$/J	Strong scattered expression throughout brain. Enriched in superficial cortical layers and restricted populations in hindbrain and midbrain.

Table 2. Reporter line crossed to Cre transgenic lines.

Reporter Line	Expressed Gene	Originating Lab or Donating Investigator	Public Repository (Stock #)	Official Strain Name	Expression Pattern Summary
Ai14	tdTomato	Allen Institute for Brain Science	The Jackson Laboratory (007914)	B6.Cg-*Gt(ROSA)26Sor*$^{tm14(CAG-tdTomato)Hze}$/J	tdTomato fluorescent protein is expressed in cytoplasm.

REFERENCES

Cauli B, Audinat E, Lambolez B, Angulo MC, Ropert N, Tsuzuki K, Hestrin S, Rossier J (1997) Molecular and physiological diversity of cortical nonpyramidal cells. *Journal of Neuroscience* 15:3894-3906.

Cauli B, Porter JT, Tsuzuki K, Lambolez B, Rossier J, Quenet B, Audinat E (2000) Classification of fusiform neocortical interneurons based on unsupervised clustering. *Proceedings of the National Academy of Sciences USA* 97:6144-6149.

Crick FHC (1994) *The Astonishing Hypothesis: The Scientific Search for the Soul*. Simon & Schuster, New York.

DeFelipe J, López-Cruz PL, Benavides-Piccione R, Bielza C, Larrañaga P, Anderson S, Burkhalter A, Cauli B, Fairén A, Feldmeyer D, Fishell G, Fitzpatrick D, Freund TF, González-Burgos G, Hestrin S, Hill S, Hof PR, Huang J, Jones EG, Kawaguchi Y, Kisvárday Z, Kubota Y, Lewis DA, Marín O, Markram H, McBain CJ, Meyer HS, Monyer H, Nelson SB, Rockland K, Rossier J, Rubenstein JL, Rudy B, Scanziani M, Shepherd GM, Sherwood CC, Staiger JF, Tamás G, Thomson A, Wang Y, Yuste R, Ascoli GA (2013) New insights into the classification and nomenclature of cortical GABAergic interneurons. *Nature Reviews Neuroscience* 14:202-216.

Druckmann S, Banitt Y, Gidon A, Schürmann F, Markram H, Segev I (2007) A novel multiple objective optimization framework for constraining conductance-based neuron models by experimental data. *Frontiers in Neuroscience* 1:7–18.

Hay E, Hill S, Schürmann F, Markram H, Segev I (2011) Models of neocortical layer 5b pyramidal cells capturing a wide range of dendritic and perisomatic active properties. *PLoS Computational Biology* 7:e1002107.

Herculano-Houzel S (2009) The human brain in numbers: a linearly scaled-up primate brain. *Frontiers in Human Neuroscience* 3: doi:10.3389/neuro.09.031.2009.

Hines ML, Carnevale NT (1997) The NEURON simulation environment. *Neural Computation* 9:1179–1209.

Langmead B, Trapnell C, Pop M, Salzberg SL (2009) Ultrafast and memory-efficient alignment of short DNA sequences to the human genome. *Genome Biology* 10:R25.

Li B, Dewey CN (2011) RSEM: accurate transcript quantification from RNA-Seq data with or without a reference genome. *BMC Bioinformatics* 12:323.

Koch C (1999) *Biophysics of Computation: Information Processing in Single Neurons.* Oxford University Press, New York.

Macosko EZ, Basu A, Satija R, Nemesh J, Shekhar K, Goldman M, Tirosh I, Bialas AR, Kamitaki N, Martersteck EM, Trombetta JJ, Weitz DA, Sanes JR, Shalek AK, Regev A, McCarroll SA (2015) Highly parallel genome-wide expression profiling of individual cells using nanoliter droplets. *Cell* 161:1202-1214.

Madisen L, Zwingman TA, Sunkin SM, Oh SW, Zariwala HA, Gu H, Ng LL, Palmiter RD, Hawrylycz MJ, Jones AR, Lein ES, Zeng H (2010) A robust and high-throughput Cre reporting and characterization system for the whole mouse brain. *Nature Neuroscience* 13:133-140.

Masland, RH (2012) The neuronal organization of the retina. *Neuron* 76**:**266-280.

Peng H, Ruan Z, Long F, Simpson JH, Myers EW (2010) V3D enables real-time 3D visualization and quantitative analysis of large-scale biological image data sets. *Nature Biotechnology* 28:348-353.

Petilla Interneuron Nomenclature Group, Ascoli GA, Alonso-Nanclares L, Anderson SA, Barrionuevo G, Benavides-Piccione R, Burkhalter A, Buzsáki G, Cauli B, Defelipe J, Fairén A, Feldmeyer D, Fishell G, Fregnac Y, Freund TF, Gardner D, Gardner EP, Goldberg JH, Helmstaedter M, Hestrin S, Karube F, Kisvárday ZF, Lambolez B, Lewis DA, Marin O, Markram H, Muñoz A, Packer A, Petersen CC, Rockland KS, Rossier J, Rudy B, Somogyi P, Staiger JF, Tamas G, Thomson AM, Toledo-Rodriguez M, Wang Y, West DC, Yuste R (2008) Petilla terminology: nomenclature of features of GABAergic interneurons of the cerebral cortex. *Nature Reviews Neuroscience* 9:557-568.

Pozzorini C, Mensi S, Hagens O, Naud R, Koch C, Gerstner W (2015) Automated high-throughput characterization of single neurons by means of simplified spiking models. *PLoS Computational Biology* 11(6):e1004275.

Stevens CF (1998) Neuronal diversity: Too many cell types for comfort? *Current Biology* 8:R708-R710.

Sugino K, Hempel CM, Miller MN, Hattox AM, Shapiro P, Wu C, Huang ZJ, Nelson SB (2006) Molecular taxonomy of major neuronal classes in the adult mouse forebrain. *Nature Neuroscience* 9**:**99-107.

Tasic B, Menon V, Nguyen TN, Kim TK, Jarsky T, Yao Z, Levi B, Gray LT, Sorensen SA, Dolbeare T, Bertagnolli D, Goldy J, Shapovalova N, Parry S, Lee C, Smith K, Bernard A, Madisen L, Sunkin SM, Hawrylycz M, Koch C, Zeng H (2016) Adult mouse cortical cell taxonomy revealed by single cell transcriptomics. *Nature Neuroscience* Jan 4. doi: 10.1038/nn.4216
Thomson AM (2010) Neocortical layer 6, a review. *Frontiers in Neuroanatomy* 4:13.

Toledo-Rodriguez M, Blumenfeld B, Wu C, Luo J, Attali B, Goodman P, Markram H (2004) Correlation maps allow neuronal electrical properties to be predicted from single-cell gene expression profiles in rat neocortex. *Cerebral Cortex* 14:1310-1327.

Zhou Z, Sorensen S, Zeng H, Hawrylycz M, Peng H (2014) Adaptive Image Enhancement for Tracing 3D Morphologies of Neurons and Brain Vasculatures*. Neuroinformatics* 1-14.

Zhou Z, Sorensen S, Peng H (2015) Neuron crawler: an automatic tracing algorithm for very large neuron images. *Proceedings of IEEE 2015 International Symposium on Biomedical Imaging: From Nano to Macro* pp.870-874.